Volume 5 Number 10 October 1978 Nucleic Acids Research

Physical properties of inner histone-DNA complexes

P.N.Bryan*, E.B.Wright, M.H.Hsie, A.L.Olins and D.E.Olins

University of Tennessee-Oak Ridge Graduate School of Biomedical Sciences, and Biology Division, Oak Ridge National Laboratory, Oak Ridge, TN 37830, USA

Received 30 June 1978

ABSTRACT

Chicken erythrocyte inner histone tetramer has been complexed with several natural and synthetic DNA duplexes by salt-gradient dialysis at various protein/DNA ratios. The resulting complexes, in low-ionic-strength buffer, have been examined by electron microscopy, circular dichroism, and thermal denaturation. Electron microscopy reveals nucleosomes (ν bodies) randomly arranged along DNA fibers, including poly(dA-dT)·poly(dA-dT), poly(dI-dC)·poly(dI-dC), but not poly(dA)·poly(dT). Circular dichroism studies showed prominent histone α-helix and "suppression" of nucleic acid ellipticity (λ>240 nm). Thermal denaturation experiments revealed Tm behavior comparable to that of H1- (or H5-) depleted chromatin. Tm III and Tm IV increased linearly with G+C% (natural DNAs), but were virtually independent of the histone/DNA ratio; therefore, the melting of nucleosomes along a DNA chain is insensitive to adjacent "spacer" DNA lengths. This suggests that Tm III and Tm IV arise from the melting of different domains of DNA associated with the core ν body.

INTRODUCTION

There is extensive evidence that the fundamental nucleosomal structure of chromatin (1,2) can be reconstructed from a mixture of dissociated histones and DNA (3–11). Based upon reconstruction experiments, it is possible to conclude that: (a) nucleosomes can form on a wide range of DNA base sequences; (b) although H3 and H4 play a central role in organizing the nucleosomal structure all inner histones must be present at equimolarity; (c) biophysical techniques can be employed to compare reconstructed and native subunits. In the present investigation we have associated inner histone tetramers (i.e., one each of H3, H4, H2A, and H2B) to various types of DNA by the salt-gradient dialysis method. Biophysical studies reveal considerable similarity between the reassociated products and H5- and H1-depleted chromatin.

METHODS

Preparation of Inner Histones and DNAs

Inner histone tetramer from chicken erythrocyte nuclei was isolated and stored

frozen as described previously (12). The isolation and storage buffer was 2 M NaCl, 10 mM Tris (pH 7.0), and 0.1 mM dithiothreitol (DTT).

A number of DNAs were obtained from commercial sources and used without additional purification: chicken blood DNA (43% G+C), Calbiochem, San Diego, California; Micrococcus (luteus) lysodeikticus DNA (72% G+C), Sigma Chemical Corp., St. Louis, Missouri; Calf thymus DNA (43.3% G+C), Clostridium perfringens DNA (29% G+C), and Escherichia coli DNA (51% G+C), Worthington Biochemical Corp., Freehold, New Jersey. T2 and T6 DNA (34% G+C) were kindly donated by E. Volkin, Biology Division, Oak Ridge National Laboratory. The synthetic DNAs poly(dA)·poly(dT), poly(dA-dT)·poly(dA-dT), and poly(dI-dC)·poly(dI-dC) were purchased from P-L Biochemicals, Inc., Milwaukee, Wisconsin.

Histone and DNA Complex Formation

Inner histone tetramer was mixed directly with native DNA at histone/DNA ratios (g/g) varying from 0 to 1.4, in 2 M NaCl, 10 mM Tris (pH 7.0), 0.1 mM DTT, 0.2 mM EDTA. The final DNA concentration of the mixture was approximately 100 µg/ml (i.e., $A_{260} \simeq 2.0$). Histone concentrations were determined from absorbance measurements of the stock solution at 278 nm with the assumption that 1 mg/ml inner histone has an $A_{278}=0.452$.

Association was accomplished with the following protocol for a step-gradient of decreasing NaCl concentration:

Step	NaCl (M)	Tris (mM) pH 7.0	DTT (mM)	EDTA (mM)	Dialysis time/step (h)
A	2.0	10.0	0.1	0.2	≥4
B	1.4	10.0	0.1	0.2	≥4
C	1.0	10.0	0.1	0.2	≥4
D	0.3	10.0	-	0.2	≥4
E	0.1	10.0	-	0.2	≥4
F	-	10.0	-	0.2	≥4
G	-	-	-	0.2	≥12

The complexes containing histone and natural DNAs were harvested and examined in 0.2 mM EDTA (pH 7.0). Complexes with the synthetic DNAs were harvested and examined after extensive dialysis (≥12 h) at step F of the protocol. At the highest input ratios of histone/DNA, the resulting complexes occasionally exhibited turbidity. These were clarified by centrifugation for 15 min at 17,000 x g.

Protein/DNA ratios in the resulting soluble complexes were measured by the spectral method of Hanlon and co-workers (13) employing the following empirical equation:

$$\text{histone/DNA ratio} = k\left[\left(\frac{A_{230}}{A_{260}}\right)_{\text{histone-DNA}} - \left(\frac{A_{230}}{A_{260}}\right)_{\text{DNA}}\right].$$

The proportionality constant, k, represents the ratio of specific absorption coefficients of DNA (260 nm) to histone (230 nm). Because of uncertainties in the specific absorbance of histone, we calibrated k by spectral measurements of isolated chicken erythrocyte necleosomes (ν_1), assuming a histone/DNA ratio $\simeq$ 1.07 (14). From this calibration, we determined that k $\simeq$ 3.0; this value is used throughout this study. The spectral method of Hanlon was shown to be linear with protein/DNA ratios (up to the point of evident light-scattering contribution to the spectra) by comparing a series of spectral measurements on samples with measurements on the same complexes by the Folin-Lowry method for protein determination.

Biophysical Techniques

The methods employed to study the resulting soluble histone-DNA complexes (i.e., electron microscopy, circular dichroism, and thermal denaturation at 260 nm) have been adequately described in previous publications from this laboratory (12,14,15).

RESULTS

Electron Microscopy of Histone–DNA Complexes

When examined by dark-field electron microscopy, soluble histone complexes with chicken DNA exhibited ν bodies apparently irregularly arranged along DNA fibers (Fig. 1). With increasing histone/DNA ratios, ν bodies appeared to be more closely packed. On the same microscope grid, polymorphism of the chromatin fibers was readily apparent: samples revealed a mixture of well-spread fibers containing nucleosomes, and clusters of tightly packed and unspread subunits. Identical results were obtained when chicken erythrocyte inner histones were complexed with the DNA of C. perfringens or M. lysodeikticus: irregular distribution of nucleosomes, and increasing density of ν bodies along fibers with increased ratios of histone/DNA. Figure 2 demonstrates that ν bodies were also seen with complexes of inner histones and poly(dA-dT)·poly(dA-

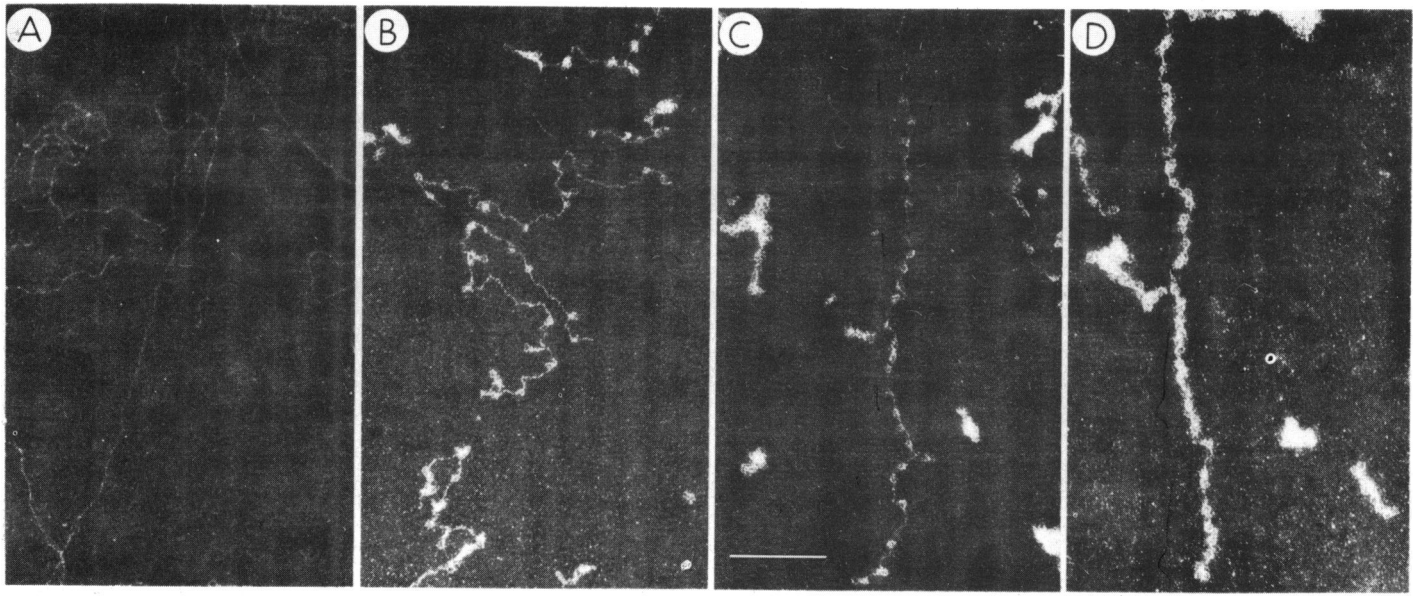

Figure 1. Dark-field electron micrographs of complexes of chicken DNA with inner histones. Samples loaded on charged carbon-coated grids without fixation, dried out of Kodak Photo-flo, and stained 30 sec with 0.1% uranyl acetate. Complexes contained the following histone/DNA ratios (g/g): (A) 0; (B) 0.41; (C) 0.85; (D) 1.04. Calibration bar corresponds to 100 nm.

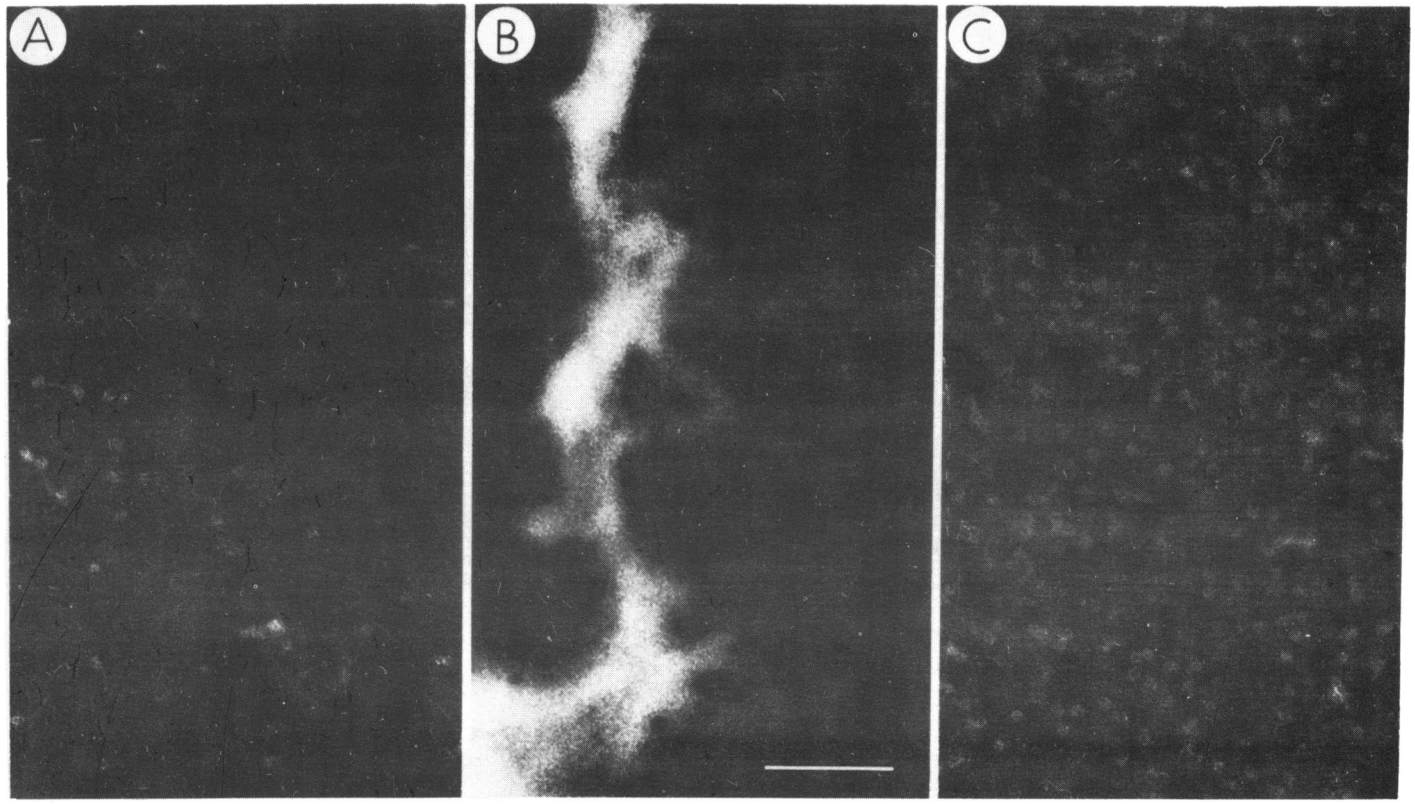

Figure 2. Dark-field electron micrographs of complexes of synthetic DNAs with inner histones. Procedures the same as in Fig. 1. Samples and histone/DNA ratios: (A) poly(dA-dT)·poly(dA-dT), 0.59; (B) poly(dA)·poly(dT), ~0.70; (C) poly(dI-dC)·poly (dI-dC), 0.59. Calibration bar corresponds to 100 nm.

dT) or poly(dI-dC)·poly(dI-dC), but not poly(dA)·poly(dT). The latter double-stranded polymer is believed to rearrange into triple-stranded complexes in buffers with high NaCl concentrations (16), which might account for its inability to form nucleosomes with added inner histones.

Circular Dichroism of Histone–DNA Complexes

Soluble complexes of chicken erythrocyte inner histones with the DNA from C. perfringens, chicken, and M. lysodeikticus were examined by circular dichroism (Fig. 3). Despite obvious differences in the spectra of the naked DNAs, increased inner histone had common consequences with all three types of DNA. With increased histone/DNA ratios: "suppression" of nucleic acid ellipticity was greater (260–300 nm), changes were minimal in part of the DNA spectra (235–260 nm), and prominent contributions from α-helix appeared (200–235 nm). Also shown in Fig. 3 is the circular dichroic spectrum of KCl-soluble ν_1 (ν_1^c) (14), which exhibits considerable similarity to the reassociated inner histone–chicken DNA complexes.

The changes in ellipticity at 280 nm (DNA conformation) and at 222 nm (α-helix contribution), as a function of histone/DNA ratio, are presented in Fig. 4. Up to histone/DNA ratios of about 0.9–1.0 the spectral changes at 280 and 222 nm are linear with histone/DNA ratio. Such results are consistent with the concept that the intrinsic spectral properties of a nucleosome (i.e., specific conformational changes in ν-body DNA, and a high proportion of histone α-helical regions) are invariant with histone/DNA ratio. The circular dichroic changes are, therefore, linear with nucleosome density, which is directly proportional to histone/DNA ratio. The data are not consistent with cooperative effects of the histone (e.g., a critical histone/DNA ratio required for α-helix formation, or alteration in DNA conformation).

Preliminary circular dichroism studies of inner histone–synthetic DNA complexes reveal similar spectral changes to those described above. This statement is complicated by the fact that the three synthetic DNA polymers employed have quite different circular dichroic spectra than natural DNAs (17). Specifically, poly(dA-dT)·poly(dA-dT) exhibited the following spectral changes with increased histone/DNA ratio: "suppression of ellipticity (255–300 nm); very little change in part of the region (240–255 nm); and appearance of α-helix contributions (200–235 nm). Poly(dI-dC)·poly(dI-dC) exhibited uniform negative shifts in the circular dichroic spectra (240–300 nm) and evidence of increased α-helix contributions (200–235 nm). Poly(dA)·poly(dT) complexes with inner

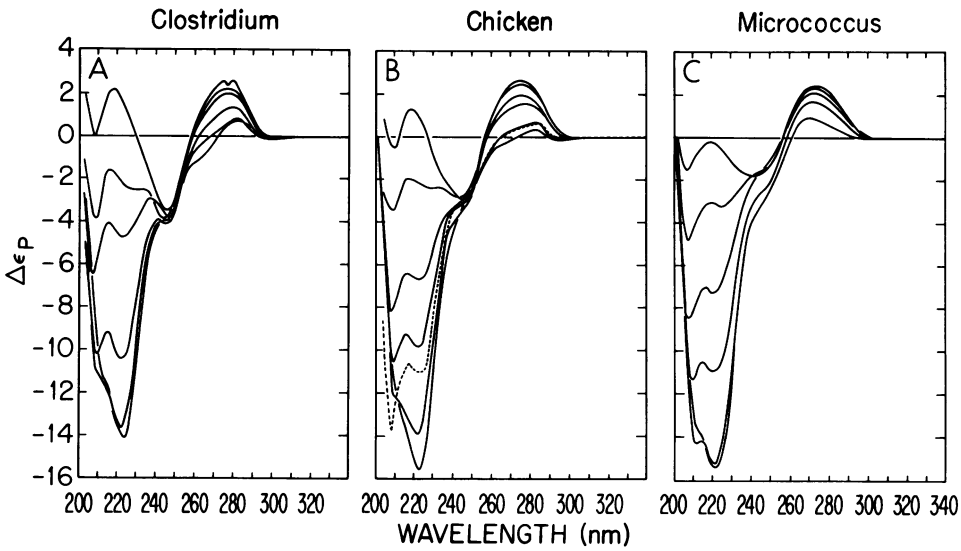

Figure 3. Circular dichroism of complexes of inner histones with different natural DNAs. The solvent for all samples was: 0.2 mM EDTA (pH 7.0). (A) C. perfringens, 29% G+C; spectra presented for the following histone/DNA ratios: 0, 0.20, 0.37, 0.66, 0.92, and 1.27. (B) Chicken DNA, 43% G+C; histone/DNA ratios: 0, 0.02, 0.37, 0.66, 0.92, and 1.27. Also presented is a representative spectrum of core nucleosomes (ν_1^c) in the same buffer (.....); histone/DNA ratio, 1.07. (C) M. lysodeikticus, 72% G+C; histone/DNA ratios: 0, 0.16, 0.35, 0.52, 0.82 and 0.97.

histones revealed no significant spectral changes in the DNA region (240–290), but showed clear evidence of histone α-helix (200–235 nm). Of the three synthetic DNA duplexes employed in the present study, the spectral changes observed with poly(dA-dT)·poly(dA-dT) most resembled those observed for natural DNAs.

Thermal Denaturation of Inner Histone–DNA Complexes

Derivative melting profiles of native and reassociated chromatin (18,19) have clearly demonstrated a number of separable thermal transitions. In low-ionic-strength buffers, comparable to those employed in the present study, chromatin or H1-depleted chromatin exhibits multiple transitions denoted (by Li et al., 18) as: I, ~47°C; II, ~57°C (a shoulder of I); III, 72°C; and IV, 82°C. The latter two transitions are generally ascribed to histone–DNA interactions (18–21), although the interpretations of their origins differ.

Thermal denaturation analysis of soluble inner histone–DNA complexes demonstrated

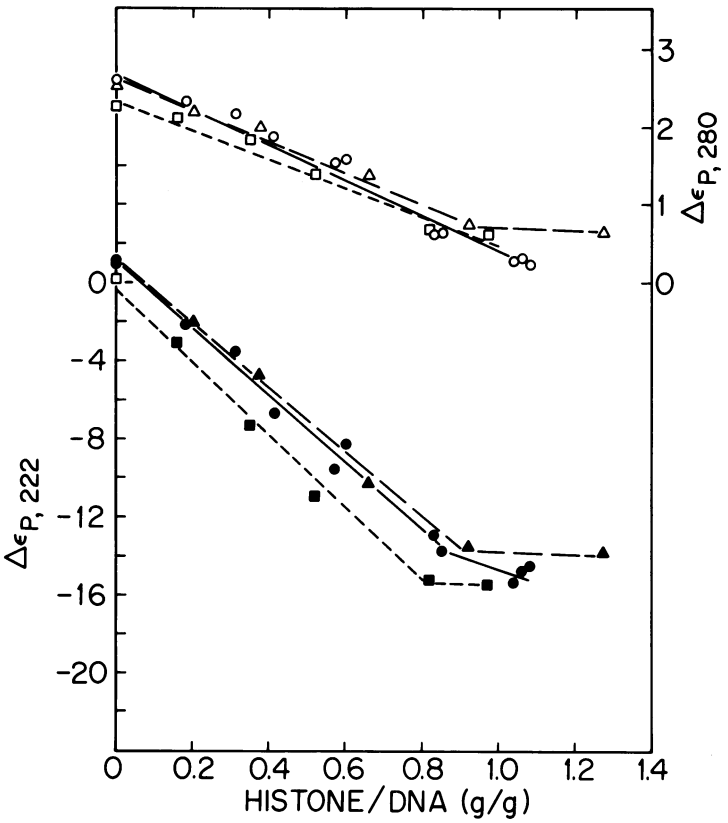

Figure 4. Relationships of $\Delta\epsilon_{p,222}$ and of $\Delta\epsilon_{p,280}$ to histone/DNA ratio, taken from the data of Fig. 3. The linear change in $\Delta\epsilon_{p,222}$ with a histone/DNA ratio of up to about 1 g/g implies that the α-helix content of the complexed histones remains constant at different histone/DNA ratios. The linear "suppression" in $\Delta\epsilon_{p,280}$ with increased histone/DNA ratios implies that any large-scale cooperative conformational effects upon the DNA are negligible. Comparative data for ν_1^c from chicken erythrocyte chromatin are also presented. Complexes are with C. perfringens (△), chicken (○), and M. Lysodeikicus (□) DNA.

considerable similarity to chromatin and to H5- and H1-depleted chromatin (see ref. 15 for previous data from this laboratory). Figure 5 presents derivative melting profiles for complexes with C. perfringens, chicken, and M. lysodeikticus DNAs. Increased histone/DNA ratios had similar effects on the melting profiles: Tm I (and II) shifted to progressively higher temperatures and decreased in hyperchromicity; Tm III and Tm IV appeared at relatively low histone/DNA ratios and did not shift significantly to higher

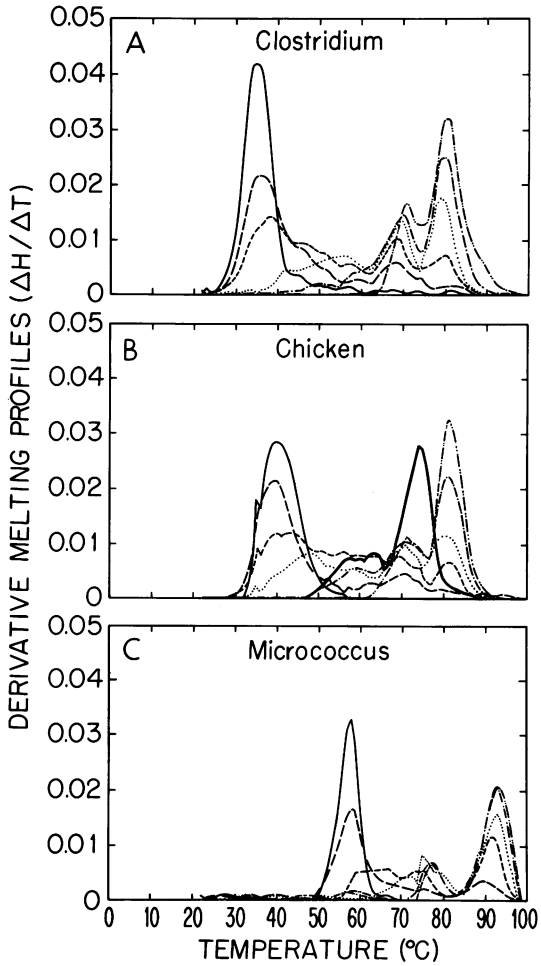

Figure 5. Derivative thermal denaturation profiles of inner histone complexes with various DNAs. Solvent for all experiments was 0.2 mM EDTA (pH 7.0). (A) C. perfringens, 29% G+C; histone/DNA ratios: 0 (——), 0.20 (— —), 0.37 (- - - -), 0.66 (····), 0.92 (— · —), and 1.27 (— ·· —). (B) Chicken DNA, 43% G+C; histone/DNA ratios: 0 (——), 0.20 (— —), 0.37 (- - - -). 0.66 (····), 0.92 (— · —), and 1.27 (— ··—). Also presented is a representative spectrum of chicken erythrocyte ν_1^c in the same buffer (.....); histone/DNA ratio, 1.07. (C) M. lysodeikticus, 72% G+C; histone/DNA ratio: 0 (——), 0.16 (— —), 0.35 (- - - -), 0.52 (·····), 0.82 (— · —), and 0.97 (—··—).

temperatures. Figure 6 summarizes these conclusions and, in addition, demonstrates that the G+C% of the DNA duplex influences the stability of the histone–DNA complex. Both Fig. 5 and Fig. 6 illustrate that Tm III and Tm IV remain virtually unchanged over

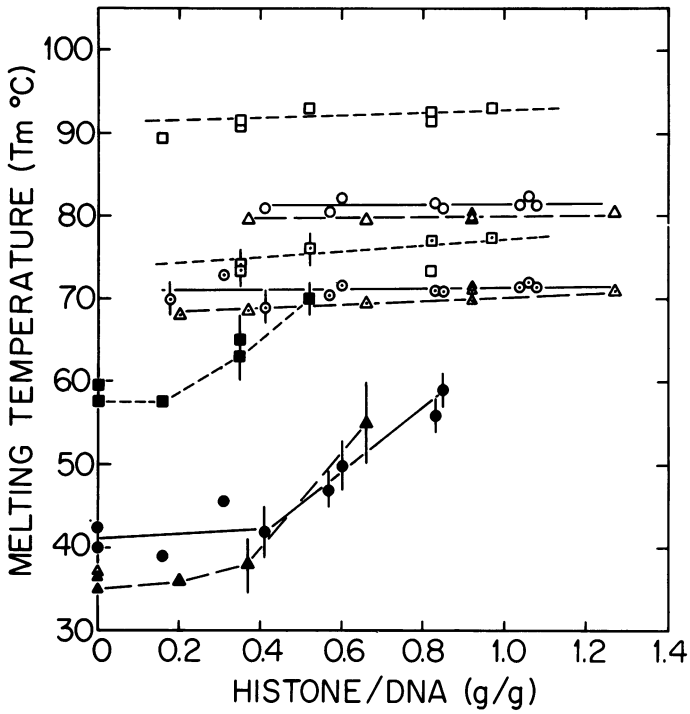

Figure 6. Melting temperatures of major transitions in histone-DNA complexes, compared at different histone/DNA ratios. Data are presented for complexes with the following DNAs: C. perfringens (△), chicken erythrocyte (○), and M. lysodeikticus (□). Major thermal transition regions are referred to by the notation of H. J. Li, as: I & II (△,○,□), III (◬,⊙,⊡), and IV (▲,●,■). Following the analysis of D. Staynov (21), we suggest that the progressive stabilization of I & II with increased histone/DNA ratios reflects the decreasing average length of naked DNA "spacers" in the h,h transitions. The minimal variance of III and IV with histone/DNA ratio implies that these transitions do not arise from different classes of ν_1 adjacent to long or short spacer regions. Rather, the data are consistent with the concept that III and IV arise from two regions of DNA with different thermal stability within each nucleosome.

a broad range of histone/DNA ratios (~0.4 to 1.0). From a comparison of these figures with the electron micrographs of Fig. 1, it is reasonsble to assume that with increased histone/DNA ratios the "spacer" regions between nucleosomes become progressively shorter, although remaining heterogeneously distributed. Thus, the progressive close-packing of ν bodies with increased histone/DNA ratios has very little influence on the thermal stability of the DNA regions associated with the histones.

We have further examined the influence of DNA G+C% upon the stability of the histone–DNA complex. Complexes were associated between inner histones and six

different DNA duplexes at histone/DNA ratios of ~0.7 – 0.8, and each complex was thermally denatured in 0.2 mM EDTA (pH 7.0). Data for Tm III and Tm IV as a function of G+C% are plotted in Fig. 7, which also illustrates data on the thermal stability of double-stranded DNA and RNA (22). Analysis of the inner histone–DNA complexes reveals an approximate linear regression of Tm III and Tm IV with G+C% in the present buffer system. To a first approximation these empirical relationships can be described as follows:

$$\text{Tm III} = 0.15(\text{G+C\%}) + 65.6$$

$$\text{Tm IV} = 0.28(\text{G+C\%}) + 71.1$$

It is of interest that the dependence of both the histone–DNA transitions on G+C% is less than that of double-stranded DNA (slope = 0.41) and RNA (slope = 0.78). The origin of this "damped" dependence of histone–DNA thermal transitions is unclear. It could result from DNA conformational changes (e.g., "C"-form DNA in association with the histones) by analogy with the difference in stabilities between double-stranded DNA and RNA. The linearity of histone–DNA thermal transitions with G+C% and the invariance of Tm with histone/DNA ratio imply that nucleosomes form at random along the DNA fiber and that melting always reflects the average G+C%.

Thermal denaturation studies on inner histone complexes with synthetic DNAs melted in 10 mM Tris, 0.2 mM EDTA (pH 7.0) demonstrated that simple-sequence DNAs exhibit two transitions analogous with Tm III and Tm IV of chromatin. Complexes with poly(dA-dT)·poly(dA-dT) were particularly well-defined, and Tm III and IV were essentially invariant with histone/DNA ratios: naked DNA melted at 52°C; Tm III, 56–57°C; and Tm IV, 67°C. It is likely, therefore, that the existence of two thermal transitions for histone–DNA interactions (i.e., Tm III and Tm IV) cannot be explained in terms of base-compositional differences between different ν bodies or regions with a single ν body.

As an essential control we tested for migration of inner histones during the melting experiments. To this end, we have mixed preformed histone–DNA complexes of high histone/DNA ratio with homologous naked DNA in 0.2 mM EDTA (pH 7.0) and have melted this mixture for comparison with complexes having the same overall histone/DNA ratio. The low-ionic-strength mixtures always exhibited the unperturbed melting of naked DNA with the expected hyperchromicity. Migration of inner histones from preformed complexes to naked DNA regions, therefore, appears unlikely in the solvent conditions employed in the present study.

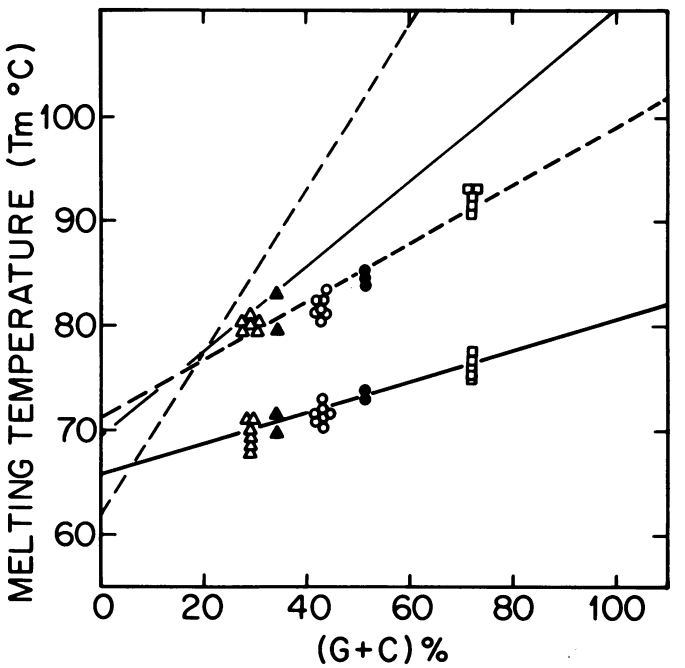

Figure 7. Dependence of thermal transitions III (——) and IV (— —) upon the average G+C% of different natural DNAs. Data are presented for the following DNAs: C. perfringens, 29% G+C; T2 and T6, 34%; chicken erythrocyte, 43%; calf thymus, 43.3%; E. coli, 51%; M. lysodeikticus, 72%. For comparative purposes, the dependence of Tm is shown for double-stranded RNA (— —) and DNA (——) upon G+C% in 0.2 M Na^+ buffers.

DISCUSSION

Employing a variety of biophysical criteria (i.e., electron microscopy, circular dichroism, and thermal denaturation), we conclude that reconstructed chromatin has a clear nucleosomal structure. The association protocol is a simple stepwise gradient of NaCl with no urea present. Because of potential H3 thiol reactivity (15), DTT was present in all buffers ≥1.0 M NaCl. It is possible to obtain good reconstruction between inner histones and DNA with a wide variety of G+C%. In principle, one can now incorporate any type of native or modified DNA (e.g., bromo-substituted, methylated, UV-irradiated, or labeled) into chromatin sturcture to examine the consequence to nucleosome conformation and stability. In preliminary studies, we have succeeded in digesting reassociated inner histone–DNA complexes with micrococcal nuclease, followed by isolation of ν_1 with the desired DNA incorporated.

The linear dependence of ellipticities at 280 nm (DNA conformation) and at 222 nm (α-helix contribution) upon histone/DNA ratios (Fig. 4) is consistent with progressive formation of ν bodies of constant spectral properties. These circular dichroic properties represent: (a) "suppressed" or C-like DNA spectra, and (b) histones consisting of ~50% α-helix (23). Inner histone complexes with poly(dA-dT)·poly(dA-dT) and with poly(dI-dC)·poly(dI-dC) exhibited a similar "suppression" of DNA ellipticities. A recent study (24) on the effects of temperature on the circular dichroic spectrum of poly(dA-dT)·poly(dA-dT) revealed similar "suppression" within the "pre-melting zone," which was interpreted as a possible B→C transition.

The thermal denaturation experiments on inner histone–DNA complexes exhibited considerable similarity to those on melting of chromatin and of H1-depleted chromatin: namely, the presence of two transitions (Tm III and Tm IV) arising from histone–DNA interaction. Staynov (21) has recently considered the possible origin of these two transitions. Three possible mechanisms were suggested: (a) ν_1 melts differently depending on whether it is adjacent to long or short spacer regions; (b) there are two classes of ν_1 (e.g., due to differences of composition and/or conformation); or (c) there are two regions of DNA stability within each nucleosome. Furthermore, Staynov suggested that current concepts of helix → coil could be applied to analyze chromatin thermal denaturation. Specifically, the following transitions were tentatively assigned: the melting of spacer DNA regions, $\underline{h},\underline{h}$ - a DNA helix "clamped" at both ends by more stable histone–DNA helices; the melting of ν, surrounded by spacers (loops) of varying length, $\underline{l},\underline{l}$; the melting of an isolated ν_1 with two free DNA ends, $\underline{O},\underline{O}$; and the melting of a terminal DNA spacer between ν_1 and an end, $\underline{O},\underline{h}$. Staynov considered the dependence of each type of transition upon increasing DNA residue length (N) and concluded that: the Tm of $\underline{h},\underline{h}$ decreases as N increases; the Tm of $\underline{O},\underline{O}$ increases with N; the Tm of $\underline{O},\underline{h}$ remains approximately constant; and the Tm of $\underline{l},\underline{l}$ generally decreases with increasing loop size—i.e., histone–DNA thermal transitions surrounded by long spacers are less stable than transitions within short spacer regions.

The present melting data on inner histone–DNA complexes at varying histone/DNA ratios can be conveniently interpreted in terms of Staynov's analysis. With increasing histone/DNA ratios, one would expect $\underline{h},\underline{h}$ regions to shorten and increase stability, in qualitative agreement with the progressive stabilization of Tm I and II. $\underline{O},\underline{h}$ transitions probably are only observable at low histone/DNA ratios. The most interesting conclusion from our data at varying histone/DNA ratios is that the influence of loop

length on I,I transitions is almost neglibible—Tm III and Tm IV remain virtually constant at different histone/DNA ratios. Indeed, these latter data strongly imply that Tm III and Tm IV are probably not due to the presence of nuclesomes within two populations of DNA spacer lengths. In addition, our preliminary data on inner histone–synthetic DNA complexes suggest that Tm III and Tm IV do not arise from DNA compositional differences. The most likely explanation, therefore, for the two higher thermal transitions of histone–DNA complexes is that there are two DNA domains of differential stability within each ν body.

In a recent thorough investigation of the thermal stability of isolated monomer nucleosomes (25), the authors document its biphasic character. Figure 5 illustrates our similar findings. Weischet et al. (25) further demonstrate that the lower DNA transition of ν_1 is reversible and does not involve simultaneous denaturation of α-helical regions, whereas, the higher transition is not reversible and does involve α-helix destruction. The fact that these two transitions are shifted down in stability from Tm III and Tm IV in the same solvent (Fig. 5) is consistent with the destabilizing effects of the DNA ends in O,O transitions. It is not possible to give a more detailed assignment of the two thermal transitions of histone–DNA complexes or of isolated ν_1 because of a fundamental uncertainty: hyperchromic changes could arise from the complete melting of localized DNA regions within the nucleosome (e.g., ends) or from a partial denaturation of all the DNA within the subunit. Whatever the exact structural origin of the biphasic melt of ν_1, it is attractive to assume that these transitions are identical to Tm III and Tm IV, but shifted to lower temperatures by the free DNA ends.

Reconstruction experiments of the type reported here are currently being extended to determine the structural role of the H1 class of histones and the consequences of histone modifications to nucleosomal conformation and stability.

ACKNOWLEDGEMENTS

This research was sponsored jointly by research grants GM 19334 (DEO) and PCM77-21498 (ALO) and the Division of Biomedical and Environmental Research, U.S. Department of Energy, under contract W-7405-eng-26 with Union Carbide Corporation. PNB is a predoctoral investigator supported by National Cancer Institute Grant CA 09104.

*To whom correspondence should be addressed

REFERENCES

1. Cold Spring Harbor Symp. Quant. Biol. (1977) 42, in press

2. Felsenfeld, G. (1978) Nature 271, 115–121
3. Olins, A. L., Carlson, R. D., and Olins, D. E. (1975) J. Cell Biol. 64, 528–537
4. Oudet, P., Gross-Bellard, M. and Chambon, P. (1975) Cell 4, 281–300
5. Garell, A., Kovacs, A. M., Champagne, M. and Daune, M. (1976) Nucleic Acids Res. 3, 2507–2520
6. Woodcock, C. L. F. (1977) Science 195, 1350–1352
7. Tatchell, K. and Van Holde, K. E. (1977) Biochemistry 16, 5295–5303
8. Leffak, I. M. and Li, H. J. (1977) Biochemistry 16, 5869–5878
9. Sollner-Webb, B., Camirini-Otero, R. D. and Felsenfeld, G. (1977) Cell 9, 179–193
10. Camerini-Otero, R. D. and Felsenfeld, G. (1977) Proc. Natl. Acad. Sci. USA, 74, 5519–5523
11. Stein, A., Bina-Stein, M. and Simpson, R. T. (1977) Proc. Natl. Acad. Sci. USA 74, 2780–2784
12. Olins, D. E., Bryan, P. N., Harrington, R. E., Hill, W. E. and Olins, A. L. (1977) Nucleic Acids Res. 4, 1911–1931
13. Johnson, R. S., Chan, A. and Hanlon, S. (1972) Biochemistry 11, 4347–4358
14. Olins, A. L., Carlson, R. D., Wright, E. B. and Olins, D. E. (1976) Nucleic Acids Res. 3, 3271–3291
15. Zama, M., Bryan, P. N., Harrington, R. E., Olins, A. L. and Olins, D. E. (1977) Cold Spring Harbor Symp. Quant. Biol. 42, in press
16. Arnott, S. Personal communication
17. Cech, C. L. and Tinoco, I. (1977) Bioplymers 16, 43–65
18. Li, H. J., Chang, C. and Weiskopf, M. (1973) Biochemistry 12, 1763–1772
19. Tsai, Y. H., Ansevin, A. T. and Hnilica, L. S. (1975) Biochemistry 14, 1257–1265
20. Hanlon, S., Johnson, R. S. and Chan, A. (1974) Biochemistry 13, 3972–3981
21. Staynov, D. Z. (1976) Nature 264, 522–525
22. Bloomfield, V. A., Crothers, D. M. and Tinoco, I. (1974) Physical Chemistry of Nucleic Acids, pp. 328–332. Harper & Row, New York
23. Thomas Jr., G. J., Prescott, B. and Olins, D. E. (1977) Science 197, 385–388
24. Brahms, S., Brahms, J. and Van Holde, K. E. (1976) Proc. Natl. Acad. Sci. USA 73, 3453–3457
25. Weischet, W. O., Tatchell, K., Van Holde, K. E. and Klump, H. (1978) Nucleic Acids Res. 5, 139–160